Atmos. Chem. Phys. Discuss., 11, 31363–31399, 2011
www.atmos-chem-phys-discuss.net/11/31363/2011/
doi:10.5194/acpd-11-31363-2011

Atmospheric Chemistry and Physics Discussions

A parameterization of low visibilities for hazy days in the North China Plain

J. Chen[1], C. S. Zhao[1], N. Ma[1], P. F. Liu[1], T. Göbel[3], E. Hallbauer[3], Z. Z. Deng[1], L. Ran[1], W. Y. Xu[1], Z. Liang[1], H. J. Liu[1], P. Yan[2,*], X. J. Zhou[1,2], and A. Wiedensohler[3]

[1]Department of Atmospheric and Oceanic Sciences, School of Physics, Peking University, Beijing, China
[2]Chinese Academy of Meteorological Sciences, China Meteorological Administration, Beijing, China
[3]Leibniz Institute for Tropospheric Research, Leipzig, Germany
[*]now at: Meteorological Observation Centre, China Meteorological Administration, Beijing, China

Received: 7 November 2011 – Accepted: 16 November 2011 – Published: 30 November 2011

Correspondence to: C. S. Zhao (zcs@pku.edu.cn)

Published by Copernicus Publications on behalf of the European Geosciences Union.

Abstract

Visibility degradation is a pervasive and urgent environmental problem in China. The occurrence of low visibility events is frequent in the North China Plain, where the aerosol loading is quite high and aerosols are strongly hygroscopic. A parameterization scheme for low visibility conditions on hazy days is proposed in this paper, based on visibility, relative humidity (RH), aerosol hygroscopic growth factors and particle number size distributions measured during the Haze in China (HaChi) Project. Observational results show that a high aerosol volume concentration is responsible for low visibility at RH < 90 %; while for RH > 90 %, decrease of visibility is mainly influenced by the increase of RH. The parameterization scheme is developed on the basis of aerosol volume concentrations and RH, taking into accounts the sensitivity of visilibity to the two factors and the availability of corresponding data. The extinction coefficients calculated with the parameterization scheme agree well with the measured values.

1 Introduction

Visibility degradation is a pervasive environmental problem in China (Anderson et al., 2003; Quinn et al., 2003; Zhao et al., 2006b; Hoyle et al., 2009). Low visibility conditions present a host of problems of human activities such as air transport and highway traffic. In the North China Plain (NCP), low visibility events are frequently encountered and mainly accompanied with haze as a result of either high aerosol loading or the strong hygroscopic growth of the aerosol particles.

Recently, China has undergone a rapid economic growth. Many regions have suffered from severe pollution caused by large amounts of aerosol particles emitted from fossil fuel and biomass burning processes, transport and some other combustion sources. High levels of particulate matter with the diameter smaller than 2.5 µm ($PM_{2.5}$) have been reported in a few megacities. Annual averages (2005–2006) of $PM_{2.5}$ in Beijing and Chongqing were $118.5 \pm 40.6\,\mu g\,m^{-3}$ and $129.0 \pm 42.6\,\mu g\,m^{-3}$,

ACPD
11, 31363–31399, 2011

respectively (Yang et al., 2011). Annual average $PM_{2.5}$ (1999–2000) in Shanghai was 67.6 $\mu g\,m^{-3}$ (Ye et al., 2003). The seasonal average in urban Guangzhou was $81.7 \pm 25.6\,\mu g\,m^{-3}$ in winter 2008 (Yang et al., 2011). Mass concentrations of $PM_{2.5}$ in Beijing and Chongqing both exceeded the national air quality standard of particulate matter within 10 µm (PM_{10}) for residential areas (100 $\mu g\,m^{-3}$) and were at least 10 times those (5–10 $\mu g\,m^{-3}$) measured in US continental east (Hidy et al., 2009). Intensive aircraft observations in Beijing showed that the average aerosol number concentration near surface level (1419 m above the ground) was about 6600 cm^{-3}, with the highest value over 10 000 cm^{-3} (Zhao et al., 2006a; Deng et al., 2009; Liu et al., 2009).

Hygroscopicity greatly affects aerosol optical properties (Covert et al., 1972; Cheng et al., 2008a; Stock et al., 2011). Hygroscopic growth would increase aerosol extinction coefficients by enlarging the particle size. On the other hand, hygroscopic growth decreases aerosol extinction coefficients by lowering the refractive index, since uptaked water has a smaller refractive index compared to other aerosol components. The positive effect of the aerosol size on aerosol extinction coefficients outweighs the negative effect of the refractive index, leading to an increase in aerosol extinction and a significant degradation in visibility, as have been observed in some field campaigns (Yan et al., 2008a; Pan et al., 2009). Measurements of ambient aerosol hygroscopic properties were conducted in the NCP using a Hygroscopicity Tandem Differential Mobility Analyser (H-TDMA) (Swietlicki et al., 2008). Corresponding observational results of the Haze in China Project (HaChi) presented that average hygroscopic growth factor of more hygroscopic particles (initial diameters of 100 nm) was about 2.45 ± 0.07 at 98.5 % relative humidity (RH) (Liu et al., 2011). This value was 0.25 lower than that of the pure ammonium sulphate particles, indicating high hygroscopicity of the ambient aerosols.

Studies regarding the trends of visibility (Deng et al., 2008; Chang et al., 2009), source apportionment of visibility impairment (Ying et al., 2004) and the correlation between visibility and its influencing factors have shown that visibility was largely influenced by the particle size distribution (Motallebi et al., 1990; Cheng et al., 2008b),

ACPD
11, 31363–31399, 2011

meteorological conditions (Wu et al., 2005; Deng et al., 2008; Zhang et al., 2010) and aerosol chemical components (Randles et al., 2004; Armin Sorooshian et al., 2008; Wen et al., 2010). An exponential correlation has been found between visibility and aerosol mass concentration (Wen et al., 2010). It has also been reported that the mixing state of black carbon (BC, i.e. soot particles) has an important effect on visibility by changing aerosol optical properties (Yu et al., 2010; Ma et al., 2011a).

Aerosol light exctinction is closely related to aerosol hygroscopic growth, which is also a key factor in visibility reduction. It is thereby of great importance to understand the correlation between low visibility, aerosol loading and aerosol hygroscopic growth. Due to frequent haze events in China, visibility is often seriously impaired (Wu et al., 2005), exerting hazardous influences on both road traffic and air transport. However, studies on visibility and its relationship with aerosol hygroscopic properties are still rather limited in China, due to the lack of aerosol hygroscopic properties measurements. In order to increase the efficiency and safety of transportation under low-visibility conditions, efforts aimed at developing a parameterization of low visibilities on hazy days are necessary for low visibility forecasts and numerical simulations. In this paper, a parameterization scheme of low visibilities for hazy days has been proposed.

This work is based on the analysis of in-situ measurements of visibility, RH, particle number size distribution (PNSD) and inferred size-resolved hygroscopic growth factors at subsaturated conditions (RH < 100 %) during the HaChi summer campaign. The characteristics of aerosol number, volume concentrations, RH and visibility are displayed in Sect. 4.1. In Sect. 4.2, results from a comparison study between the Mie model calculated and measured extinction coefficients (K_{ex}) are shown. The theretical calculation of K_{ex}, as well as the dependence of K_{ex} on aerosol volume concentration, PNSD pattern and RH are discussed in Sect. 4.3. Finally, a parameterization scheme of low visibilities under hazy conditions is presented in Sect. 4.4.

ACPD
11, 31363–31399, 2011

2 Measurement

2.1 Site description

The HaChi summer campaign was carried out at the Wuqing Meteorological Station (39°23′ N, 117°01′ E, 7.4 m a.s.l.), northwest of the Wuqing town. Wuqing is a suburban district of Tianjin (with about 0.8 million inhabitants) and located among a cluster of cities. The Wuqing town is about 80 km to the southeast of the megacity Beijing and 30 km to the northwest of the megacity Tianjin. The surrounding area of the site is in agricultural, residential and industrial land use. Most of the neighboring factories are clustered to the east of the site. While a large tract of farmland is situated to the west and south of Wuqing, with railways and busy roads running through. Wuqing is highly representative of regional aerosol pollution in the NCP and is an ideal place for our study.

2.2 Instruments and data processing

The HaChi summer campaign took place from 13 July to 14 August 2009. Ground-level aerosol particle number size distribution (PNSD), hygroscopicity, chemical composition, optical properties, visibility and RH were measured during the entire field campaign.

A combined system of Twin Differential Mobility Particle Sizer (TDMPS, Leibniz-Institute for Tropospheric Research (IfT), Germany; Birmili et al., 1999) and Aerodynamic Particle Sizer (APS, TSI Inc., Model 3320) is used to monitor the PNSDs ranging from 3 nm to 10 µm in dry condition (RH < 30 %) every 10 min. PNSDs with electrical mobility diameters ranging from 3 to 800 nm were measured by TDMPS. PNSDs with aerodynamic diameters ranging from 500 nm to 10 µm were measured by APS. More information about the two instruments is in Ma's study on aerosol optical properties in the NCP (Ma et al., 2011b).

ACPD
11, 31363–31399, 2011

The High Humidity Tandem Differential Mobility Analyser (HH-TDMA) was applied to measure the size-resolved hygroscopic growth factors of the ambient aerosols (initial diameters, D_p, are 50, 100, 200 and 250 nm) at 90 %, 95 % and 98.5 % RH (Hennig et al., 2005). More details of the instrument and observational aerosol hygroscopic properties are described in Liu et al. (2011).

Visibility was detected with a forward scattering measuring visibility meter (Model FD 12, Vaisala Corporation, Finland). Instantaneous visibilities at a temporal resolution of 15 s are further averaged into 1-min averages. Corresponding K_{ex} could be calculated from visibility according to following equation provided by the Vaisala Visibility Meter User's Guide (Visibility Meter FD12P User's Guide, 2002):

$$K_{ex}(\mathrm{km}^{-1}) = \frac{3}{\mathrm{VIS\,(km)}} \quad (1)$$

To match the ten-minute PNSDs data, one-minute meteorological parameters were also averaged into ten-minute averages when missing data less than 40 %. Since we focued on low visibility during hazy days, all data during 0–12 h on 11 August, when a heavy fog event occurred, were excluded from the dataset.

3 Methodology for K_{ex} calculation

In this section, a brief introduction to K_{ex} calculation is presented. K_{ex} at different RHs and aerosol volume concentrations can be theoretically obtained by using averaged PNSD and the Mie model, in which aerosol hygroscopic growth has been taken into account. Size-resolved hygroscopic growth factors are determined by using a combination of a four-mode PNSD fitting and HHTDMA-measured hygroscopicity parameter k at four specific particle sizes. Then follows the size-resolved refractive indices need to be considered in the Mie model. Section 3.3 is a brief introduction to the Mie model.

ACPD
11, 31363–31399, 2011

3.1 Size-resolved hygroscopic growth factors ($f(D_p, RH)$)

High aerosol hygroscopicity would greatly degrade visibility due to increasing light extinction of growing particles. The hygroscopic growth factor ($f(D_p, RH)$) is often adopted to describe aerosol hygroscopicity and defined as a function of RH:

$$f(D_p, RH) = D_p(RH)/D_{p,dry} \quad (2)$$

where $D_p(RH)$ and $D_{p,dry}$ are particle diameters under humid and dry conditions, respectively.

Size-resolved hygroscopic growth factors for aerosols within the range of 3 nm–10 µm were obtained from the measured PNSDs and HHTDMA-determined hygroscopicity parameter κ during the summer campaign. Firstly, the meansured PNSDs were fitted with four lognormal modes (Whitby, 1978; Birmili, 2001; Hussein, 2005), a nucleation mode with geometric mean diameters between 3 and 25 nm, an Aitken mode with geometric mean diameters between 25 and 100 nm, an accumulation mode with geometric mean diameters between 100 nm and 1 µm, and a coarse mode with geometric mean diameters between 1 and 5 µm. Based on the assumption that aerosols in a specific mode have common sources or have experienced similar aging processes, the corresponding hygroscopicity parameter κ in a mode should be the same due to the common chemical compositions. Hence, combined with the HHTDMA-measured hygroscopicity parameter κ of particles with diameters of 50, 100, 200 and 250 nm, the four-mode PNSD fitting method can be used to estimate the size-resolved κ for aerosols with diameters in the range of 3 nm–10 µm (Ma et al., 2011). Accordingly, the size-resolved hygroscopic growth factors at different RHs can be derived from the size-resolved κ using following equation in Petters et al. (2007):

$$RH = \frac{gf^3 - 1}{gf^3 - (1-\kappa)} \cdot \exp\left(\frac{4\sigma_{s/a} \cdot M_w}{R \cdot T \cdot D_d \cdot gf}\right) \quad (3)$$

where $\sigma_{s/a}$ is the surface tension of the solution/air interface, M_w is the molecular weight of water, R is the universal gas constant, T is temperature, D_d is the dry particle

ACPD
11, 31363–31399, 2011

diameter, and gf is the aerosol hygroscopic growth factor.

Figure 1 displays the averaged size-resolved hygroscopic growth factors at 80 %, 90 %, 95 %, 98.5 % and 99 % RH. Mean values of HHTDMA-measured hygroscopic growth factors (with dry diameters of 50, 100, 200 and 250 nm) at RHs of 90 %, 95 % and 98.5 % were shown in colored circles; error bars stand for the standard deviation (Liu et al., 2011). It can be clearly seen that the hygroscopic growth factors of particles with diameters between 50 nm and 1 µm are all higher than 1.25 at 80 % RH, significantly higher than that of the other sizes. The hygroscopic growth factors of particles larger than 2 µm are exclusively close to 1.0, given the principal chemical compositions in coarse mode are assumed to be hydrophobic mineral dust. Differences of hygroscopic growth factors for different particle sizes are larger when the RH level is higher. The hygroscopic growth factor of particles in a range of 200 nm to 1 µm is higher than 1.5 at 90 % RH, and nearly 2.0 at 95 % RH. The hygroscopic growth factors of particles within the range of 50 nm–1 µm are exclusively higher than 2.0 when RH = 99 %, and those of particles ranging from 250 nm to 1 µm even exceed 3.0. It indicates high aerosol hygroscopicity in the NCP, which has been supported by HHTDMA measurements during the HaChi campaign. Averaged hygroscopic growth factor of more hygroscopic particles with dry diameter of 100 nm was reported as 2.45 ± 0.07 at 98.5 % RH in Liu et al. (2011). This value is comparable to that ($f_{(NH_4)_2SO_4}^{(100\,nm,98.5\%)} = 2.75$) of pure ammonium sulphate particles.

Hygroscopic growth of aerosols leads to a change in particle size distribution. It is feasible to calculate the ambient PNSDs at any specific RH using PNSDs measured in dry condition and the mean size-resolved hygroscopic growth factors.

3.2 Size-resolved refractive indices ($\tilde{m}(D_{p,RH})$)

Size-resolved refractive indices are key factors in accurately calculating extinction coefficients with the Mie model. A two-component optical aerosol model of light-absorbing BC and non-light-absorbing components (Wex et al., 2002; Cheng et al., 2006) is used

ACPD
11, 31363–31399, 2011

for determining the optical equilibrium refractive index for dry particles ($\tilde{m}_p$). In this paper, dry particle is assumed to be a completely internal mixture of BC. The refractive index for dry particles is derived as a volume-weighted average between BC and non-light-absorbing components:

$$\tilde{m}_p = f_{\mathrm{BC,V}} \cdot \tilde{m}_{\mathrm{BC}} + (1 - f_{\mathrm{BC,V}}) \cdot \tilde{m}_{\mathrm{non}} \quad (4)$$

where $\tilde{m}_{\mathrm{BC}}$ and $\tilde{m}_{\mathrm{non}}$ are the refractive indices, respectively for BC and non-absorbing component, which are set to be $1.96 - 0.66i$ (Seinfeld and Pandis, 1998) and $1.53 - 10^{-7}i$ (Wex et al., 2002). $f_{\mathrm{BC,V}}$ stands for the volume fraction of BC and can be expressed as:

$$f_{\mathrm{BC,V}} = \frac{m_{\mathrm{BC}}/\rho_{\mathrm{BC}}}{V_{\mathrm{PNSD}}} \quad (5)$$

where V_{PNSD} is the corresponding aerosol volume concentration of each measured PNSD during the HaChi campaigns. m_{BC} represents the total mass concentration of BC, and ρ_{BC} is the density of BC. The total mass concentration of BC is obtained from measurements during the HaChi campaigns in spring and summer 2009 at Wuqing. Based on the reported BC-density range of 1.00–2.00 g cm^{-3} (Ouimette and Flagan, 1982; Sloane et al., 1983, 1984; Seinfeld and Pandis, 1998), an average value of 1.5 g cm^{-3} (Ma et al., 2011b) is adopted. The volume fractions of BC and the corresponding refractive indices for dry particles can be calculated using Eqs. (5) and (4).

Our results show that the mean refractive indices for dry particles are $1.558 - 0.043i$ for spring 2009 and $1.562 - 0.049i$ for summer 2009. Their corresponding standard deviations in the two seasons were $0.009 - 0.014i$ and $0.010 - 0.016i$, respectively. It indicates that in-situ observational optical equilibrium refractive indices for dry particles slightly vary with the volume fractions of BC. Possible influences of different refractive indices of dry particles on extinction coefficients are also discussed using the mean PNSD with the Mie model. The average percentage deviations of aerosol extinction coefficients, namely, the ratios between the standard deviations and mean values of calculated extinction coefficients during the two campaigns, are typically less than 3 % (for

ACPD
11, 31363–31399, 2011

spring) and 1 % (for summer). This is consistent with the results of Lesins et al. (2002). The mean value of the refractive indices during the two seasons is thereby taken as the equilibrium refractive index for dry particles, with $\tilde{m}_p = 1.56 - 0.045i$.

In humid condition, uptaked water content should be taken into consideration for refractive indices. The size-resolved refractive index for internally mixed aerosols is derived as a simple volume-weighted average between the refractive indices of dry particles and water component. The refractive index for pure water is $\tilde{m}_w = 1.33 - 0i$ (Seinfeld and Pandis, 1998). The volume of ambient PNSDs ($V_{PNSD,RH}$) in each size bin can be derived from dry PNSDs by considering aerosol hygroscopic growth. The size-resolved volume of uptaked water (V_w) can be equivalently expressed as the difference of volumes ($V_{PNSD,RH} - V_{PNSD,dry}$) between ambient and dry PNSDs ($V_{PNSD,dry}$) in each size bin. The size-resolved volume fraction of water content ($f(\log D_p)_{w,V}$) is defined as $f(\log D_p)_{w,V} = V_w / V_{PNSD,RH}$. Similarly, the size-resolved refractive index ($\tilde{m}(D_{p,RH})$) can be expressed as a volume-weighted average between the two components:

$$\tilde{m}(D_{p,RH}) = (1 - f(\log D_p)_{w,V}) \cdot \tilde{m}_p + f(\log D_p)_{w,V} \cdot \tilde{m}_w \quad (6)$$

3.3 Mie model

The Mie model is employed to calculate major optical parameters of a spherical particle, such as scattering, absorption and extinction cross sections (σ_{sc}, σ_{ab}, σ_{ex}) and scattering phase function (P_θ). Calculations in the Mie model are based on the Mie theory (Mie et al., 1908). Key parameters can be determined by particle size parameter x and the complex reflective index $\tilde{m}$ following the Bohren-Huffman Mie model (BHMIE) (Bohren and Huffman, 1983).

$$x = 2\pi r / \lambda \quad (7)$$

$$\tilde{m} = n_r + n_i \quad (8)$$

Where r is the particle size, and λ represents the wavelength of incident light. n_r and n_i are the real and imaginary part of the reflective index, representative of the scattering and absorption item, respectively. They are wavelength-dependent and nonnegative.

ACPD
11, 31363–31399, 2011

Based on size-resolved hygroscopic growth factors provided in Sect. 3.1 and size-resolved refractive indices in Sect. 3.2, the K_{ex} for each size bin can be calculated by using the BHMIE model at a given RH in the subsaturated ambient atmospheric. Total K_{ex} of the PNSDs is derived by using the aerosol number concentration at each size bin, which is constant before and after hygroscopic growth.

$$K_{ex} = \int_0^\infty \sigma_{ex}(r) n(r) dr = \sum_r \sigma_{ex}(r) * dN \quad (9)$$

4 Results and discussion

4.1 Characteristics of visibility, aerosol number concentration, volume concentration and RH

The occurrence frequencies (Freq, in %) of five specific visibility ranges are shown in Table 1. The frequency of VIS < 10 km reaches up to 89.5 %. The frequencies of VIS < 3 km and VIS < 1 km exceed 50 % and 10 %, respectively. During the valid 24-day observational period, 470 h in total experienced a low visibility (VIS < 10 km). On average, visibilities below 3 km occurred for more than 10 h each day. It was evident that the NCP frequently suffered from severe low visibility events.

The statistical results of visibility (VIS), aerosol number (N), surface (S) and volume (V) concentrations, as well as the effective radius (R_{eff}) and RH in the NCP are given in Table 2. As can be seen from the corresponding minimum (Min) and maximum (Max) values, all of the parameters show a wide range. The average visibility is only 4.145 km, with the lowest value of about 21 m. Aerosol number concentrations range from 3350–51 060 cm^{-3}, with the average level exceeding 17 000 cm^{-3}. While the mean value of particles larger than 100 nm is even higher than 5300 cm^{-3}, indicating heavy aerosol pollution in the NCP. The high aerosol surface and volume concentrations also confirm the aerosol polluted status. This has also been demonstrated by Ma et al. (2011b), in

ACPD
11, 31363–31399, 2011

which high average scattering coefficients ($\sigma_{sp,550\,nm}$) of $874 \pm 282\,Mm^{-1}$ were observed during two heavily polluted episodes in 2009 summer. The effective aerosol radii were mainly distributed in the range of 104–437 nm, with a mean value of 191.8 nm. Observed RH varied from 28 % to 100 %, with a high average value of 81.6 %. Humid weather conditions are common in the NCP during summertime.

To gain more insight into correlations between low visibility and its influencing factors, RH, aerosol number and volume concentrations were avaraged into bins. RH was divided into 7 bins, with RH < 40 % as a single bin and RH from 40 % to 100 % being divided into bins of 10 % interval. Aerosol number and calculated volume concentrations were both divided into 20 even bins, with the concentrations ranging from 0–50 000 cm^{-3} and 0–250 $\mu m^3\,cm^{-3}$, respectively. Visibility data were also sorted according to the bins of above parameters. The occurrence frequency of the visibility for each bin was calculated for five ranges (VIS ≥ 10 km, 5 km ≤ VIS < 10 km, 3 km ≤ VIS < 5 km, 1 km ≤ VIS < 3 km and VIS < 1 km). The stacked colored bars in Fig. 2 show percentages of five specific visibility groups for different ranges of aerosol volume concentration, number concentration and RH. The probability distribution functions (PDF) of aerosol volume concentration, number concentration and RH were calculated and correspondingly displayed in dotted dark lines. The PDF was defined as the proportion that the data in a specific range took among all the in-situ observations.

The frequencies of different low visibility ranges irregularly vary with increasing aerosol number concentrations in Fig. 2b. Low visibility can occur under different aerosol number concentrations, indicating that the aerosol number concentration is not a controlling factor of visibility degradation. However, the percentages of the five visibility groups increase sharply with growing aerosol volume concentrations and RH. For aerosol volume concentrations higher than 75 $\mu m^3\,cm^{-3}$ or RH exceeding 90 %, over 90 % of the visibilities are below 5 km. When aerosol volume concentrations are higher than 100 $\mu m^3\,cm^{-3}$ or RH > 90 %, about 85 % of the visibilities are below 3 km. This is in accordance with the statistical results of the highly frequent low visibility events in Table 1. The occurrence probability of RH ≥ 90 % is higher than 40 % (Fig. 2c), while

ACPD
11, 31363–31399, 2011

the probability of high aerosol volume concentration over 100 $\mu m^3\,cm^{-3}$ is no more than 20 % (Fig. 2a). Aerosol volume concentration of about 60 $\mu m^3\,cm^{-3}$ has the highest probability of occurrence and is regarded here as the average pollution level in the NCP. Because a high RH is more frequently observed than high volume concentrations, it should be the critical influencing factor of low visibility in this region.

Figure 2 also reaveals that VIS < 3 km and VIS < 1 km can occur at RHs < 50 % and < 80 %, respectively. The visibility degradation at relatively low RH results from severe aerosol pollution. At lower aerosol volume concentrations on the other hand, aerosol hygroscopic growth at high RH has the key effect on visibility reduction. Most of the extremely low visibility events (VIS < 1 km) in the NCP are encountered due to the concurrence of heavy aerosol pollution and strong hygroscopic growth at high RH, which leads to the occurrence of haze.

As noted above, extremely low visibility could occur at high humidity even if the aerosol volume concentration may be quite low. To confirm this assumption, sensitivity tests on correlations between visibility, RH and aerosol volume concentration are conducted in Sect. 4.3.

The aerosol volume concentration has been chosen for sensitivity tests. The volume concentration is representative of the aerosol pollution and much easier to be measured compared to the aerosol number or surface concentration, since the volume concentration is closely related to the mass concentration and can be derived from the mass concentration divided by an average particle density of 1.7 $g\,cm^{-3}$ (Wehner et al., 2008). In contrast to insufficient PNSD measurements, long-term measurements of aerosol mass concentration are common in China. Therefore, aerosol volume concentration is used in the parameterization scheme in Sect. 4.4.

ACPD
11, 31363–31399, 2011

4.2 Comparison between measured K_{ex} values and those calculated from ambient PNSDs

A comparison study of K_{ex} based on the Mie calculations and the field measurements is summarized in this section. Using the inferred mean size-resolved hygroscopic growth factors and dry PNSDs, the ambient PNSDs can be obtained according to the method stated in Sect. 3.1. The K_{ex} of the ambient PNSDs is calculated by the Mie model, while measured K_{ex} is obtained from visibility measurements. A comparison between the measured K_{ex} values and those calculated from ambient PNSDs has been made.

Figure 3 shows the comparison between calculated and measured K_{ex}. The majority of K_{ex} is clustered near the 1 : 1 line for $K_{ex} < 1000\,Mm^{-1}$ ($lg(K_{ex}) < 3.0$, lg corresponds to log_{10}), without significant systematic deviations. Corresponding RHs are mostly below 90 %. For $K_{ex} > 1000\,Mm^{-1}$ (VIS < 3 km), the dispersion of K_{ex} gradually increases, and most of corresponding RHs are higher than 90 %. This reveals that the aerosol hygroscopicity would greatly influence the variation of K_{ex} and result in large deviations. Generally, the K_{ex} calculated from ambient PNSDs agree with the measured values, with a correlation coefficient higher than 0.9 ($R^2 = 0.86966$).

The deviations in the comparison could come from two aspects. On the one hand, the visibility meter used for the in-situ measurement of K_{ex} has uncertainties. Due to the possible influence of the forward scattering angle, particle size, source wavelength and site climatology, the systematic error of the visibility sensor is reported to be larger than 10 % (Crosby, 2003). On the other hand, K_{ex} calculated from ambient PNSDs also bear uncertainties. Size-resolved hygroscopic growth factors vary with time, using the mean growth factors would cause certain deviation, the mean level of which is estimated as no higher than 10 %. Another important factor is the RH, which is also closely related to the aerosol hygroscopic growth factors. Tests reveal that the sensitivity of K_{ex} to RH variation is very high. That is, if increasing RH by 1 % ($\Delta RH = 1\,\%$) at a specific RH, the corresponding growth rates of K_{ex} (ΔK_{ex}) by using a fixed PNSD in the Mie model can be of great variation. At RH < 90 %, the ΔK_{ex} is within 10 %; while at RH > 90 %,

ACPD
11, 31363–31399, 2011

the ΔK_{ex} increases sharply. When RH grows above 95 %, the ΔK_{ex} would even exceed 20 %. It indicates that RH itself is of large uncertainty, and a tiny variation of RH can largely influence the value of K_{ex}, especially at RH > 90 %. Therefore, ensuring the accuracy of the measured RH, particularly under high RH conditions, is very critical for both field campaigns and numerical simulations. Additionally, the mixing state of black carbon can induce uncertainty to the size-resolved refractive indices and result in the deviation of K_{ex} calculation. The standard deviations of the PNSD measurements in both particle size and number concentration (Wex et al., 2002; Wiedensohler et al., 2011) also contribute to the uncertainties of the calculated K_{ex}. The overall uncertainty of the calculation with the Mie model is estimated as 34 %.

Briefly, due to the standard deviations derived from the visibility, RH and PNSD measurements, combined with the uncertainties of the K_{ex} calculation induced by the size-resolved hygroscopic growth factors and the mixing state of black carbon, discrepancies between the K_{ex} calculated from ambient PNSDs and the measured values are inevitable. The results of the comparison are confirmed to be of acceptable range. The results also prove the reliability of our in-situ observations, including the inferred size-resolved hygroscopic growth factors. They also confirm that it is appropriate to apply the inferred size-resolved hygroscopic growth factors in the Mie model for the theoretical calculation of K_{ex} in this paper.

4.3 Dependence of K_{ex} on RH volume concentration and PNSD patterns

4.3.1 Dependence of K_{ex} on RH and volume concentration

Visibility can be converted from K_{ex} according to the User's Guide of the Visibility Meter (Eq. 1), thus K_{ex} is taken as the proxy for visibility. Taking aerosol hygroscopic growth into consideration, K_{ex} at given RH and aerosol volume concentrations was calculated with the Mie model using the average PNSD. Consequently, correlations between K_{ex} (in log scale), RH and aerosol volume concentration are presented as is shown in Fig. 4b. The PDFs of aerosol volume concentration and RH are also displayed in Fig. 4a,c.

ACPD
11, 31363–31399, 2011

In Fig. 4b, it should be noted that K_{ex} generally increases with volume concentration, with the corresponding colors transforming from lower values (dark blue) to higher values (yellow). At RH < 80 %, K_{ex} is more sensitive to the variation of aerosol volume concentrationrather than to the increase of RH. This reveals the predominant influence of aerosol loading on visibility degradation at relatively low RH (RH < 80 %). At RH above 80 %, K_{ex} increases more sharply with RH than with the aerosol volume concentration. Under very humid conditions of RH > 90 %, the dominant role of aerosol hygroscopic growth in visibility impairment at high RH is even more evident.

Figure 4a shows the PDF of measured aerosol volume concentrations. About 80 % of the aerosol volume concentrations are within 100 $\mu m^3\,cm^{-3}$. The aerosol volume concentration with the largest PDF (13 %) is about 55–65 $\mu m^3\,cm^{-3}$, far below the observed maximum value (233.89 $\mu m^3\,cm^{-3}$). The aerosol volume concentrations barely reached over 200 $\mu m^3\,cm^{-3}$ in the in-situ observations. Nonetheless, the high volume concentrations over 200 $\mu m^3\,cm^{-3}$ may still occur under certain weather conditions such as a calm and stable high pressure system. The occurrence frequency of high aerosol volume concentration events depends on synoptic conditions.

In contrast to the low frequency of high aerosol volume concentrations, the PDF of RH seems to be more uniformly distributed at higher RH ranges as is shown in Fig. 4c. The probability of RH < 50 % is within 10 %. The occurrence frequency of RH ≥ 80 % are higher than 40 %, and that of RH ≥ 95 % reaches 16 %. Generally, the occurrence probability of RH gradually increases with RH. The large PDF (over 35 %) of RH > 85 % demonstrates that high RH conditions frequently occurred during this summer campaign.

The crossed area with the largest aerosol volume concentration PDF and RH PDF in Fig. 4b represents the most common aerosol pollution and humidity state in the NCP. Low visibilities under such conditions rarely fall below 1 km, which agrees well with the field observations, in which the low visibility range shows the highest occurrence frequency at 1–3 km. Visibilities in that range are determined by the combined influence of aerosol volume concentration and aerosol hygroscopic growth. When extremely low

ACPD
11, 31363–31399, 2011

visibility events (VIS < 1 km, corresponding to $\lg(K_{ex}) \geq 3.5$) occur, there is either high aerosol volume concentration or high RH. Should VIS < 1 km occurre under RH below 80 %, the corresponding aerosol volume concentrations would have to be higher than 200 $\mu m^3\,cm^{-3}$. However, it is evident that the aerosol volume concentrations rarely exceed 200 $\mu m^3\,cm^{-3}$ (with a probability below 2 %). Thus, extremely low visibility can hardly occur at low RH. On the other hand, should VIS < 1 km occurr at aerosol volume concentrations below 100 $\mu m^3\,cm^{-3}$, the corresponding RH would have to be above 95 %. The occurrence probability of RH > 95 % is higher than 16 %, which indicates that the high RH should be the predominant factor leading to extremely low visibilities at the average aerosol pollution level (as defined in Sect. 4.1).

In general, at RH below 90 %, the influence of aerosol volume concentration on K_{ex} dominates. While at RH above 90 %, RH becomes the predominant factor controlling K_{ex}. In most cases, visibility degradation is caused by the concurrence of aerosol pollution and hygroscopic growth at high RH.

4.3.2 Dependence of K_{ex} on RH and PNSD patterns

Results in Sect. 4.3.1 were derived from an average PNSD. In real-time observations, PNSDs are of temporal and spatial variations.The same aerosol volume concentration may correspond to different PNSD patterns. To test the sensitivity of K_{ex} to the PNSD patterns, the concept of aerosol volume extinction coefficient (K_{ex-vol}) is introduced, which refers to the K_{ex} at unit aerosol volume concentration. In this way, the influence of aerosol volume concentration can be excluded. The variation of K_{ex-vol} reflects the influence of PNSD patterns on aerosol light extinction at varying RH.

Taking into consideration aerosol hygroscopic growth at subsaturated conditions in the Mie model, the K_{ex-vol} of all the measured PNSDs at each RH were obtained (Fig. 5). The green, blue and red circled lines, respectively represent the average, the 5th and 95th percentile of K_{ex-vol} (K^{5th}_{ex-vol} and K^{95th}_{ex-vol}) under corresponding RH. The magenta line represents the relative deviation of K_{ex-vol} defined as (K^{95th}_{ex-vol}–

ACPD
11, 31363–31399, 2011

$K_{ex-vol}^{5th})/K_{ex-vol}^{95th}$. The relative deviation is representative of the influence of the PNSD patterns on K_{ex}.

Notably, an exponential correlation exists between the K_{ex-vol} and RH. All three lines of K_{ex-vol} increase slowly with RH at relatively low RH (RH < 80 %), K_{ex-vol} varies between 5 and 15 Mm^{-1} $(\mu m^3\,cm^{-3})^{-1}$. The relative deviation at low RH also increases slowly but nearly keeps steady near 26.5 %. This indicates that the weak hygroscopic growth at low RH can hardly affect the K_{ex-vol}. The variation of the relative deviation is smaller than 1 %. PNSD patterns have little influence on K_{ex-vol} at low RH. At RH > 90 %, the absolute deviations of K_{ex-vol} ($|K_{ex-vol}^{95th} - K_{ex-vol}^{5th}|$) increases sharply with RH. The K_{ex-vol}^{5th} and K_{ex-vol}^{95th} are larger than 25 Mm^{-1} $(\mu m^3\,cm^{-3})^{-1}$ at 95 % RH, and they both exceed 75 Mm^{-1} $(\mu m^3\,cm^{-3})^{-1}$ at 99 % RH. The hygroscopic growth at high RH greatly increases the light extinction by shifting the peaks of PNSDs to larger size bins, which have higher extinction efficiencies. Consequently, the PNSD patterns can affect the absolute deviations of K_{ex-vol} at high RH. However, the relative deviation gradually reduced by 2.5 % with RH growing from 80 % to 99 %. Therefore, the PNSD patterns can influence the light extinction to some extent. The absolute deviations of K_{ex-vol} caused by PNSD patterns vary with RH.

Generally, the sensitivity studies show that PNSD patterns have little influence on the K_{ex-vol} at RH below 80 %, with the relative deviation of K_{ex-vol} varying no more than 1 %. At RH over 90 %, PNSD patterns can slightly influence the K_{ex-vol}, with a largest reduction of the relative difference between K_{ex-vol}^{95th} and K_{ex-vol}^{5th} reaching 2.5 %. The absolute deviations between K_{ex-vol}^{95th} and K_{ex-vol}^{5th} are dominated by RH. The measurements of aerosol hygroscopicity are not only critical to the accuracy of size-resolved hygroscopic growth factors but also to the variation of extinction coefficients at unit aerosol volume concentration. Since PNSD patterns only have slight influences on K_{ex-vol}, it should be appropriate to use an average PNSD in the Mie model to calculate K_{ex}. With given aerosol volume concentration and RH, K_{ex} can be estimated from Fig. 4b.

ACPD
11, 31363–31399, 2011

4.4 A parameterization scheme for K_{ex} calculation

In the previous sections, low visibility and its influencing factors are analyzed in the NCP. Statistics show that more than half of the visibility records are below 3 km, and over 10 % are extremely low visibilities of VIS < 1 km. The low visibility events in the NCP are frequently encountered and mostly accompanied with haze due to the concurrence of heavy aerosol pollution and strong hygroscopic growth at high RH. To reduce the costs of low-visibility-related accidents and to reduce delays at airports, parameterization of low visibilities on hazy days is of practical importance.

Based on the sensitivity study in Sect. 4.3, a parameterization scheme for K_{ex} is set up. In consideration of the influence of aerosol hygroscopic growth in humid condition on the light extinction, RH is chosen as one of the factors for the parameterization. Instead of PNSD, aerosol volume concentration is chosen as the other parameter, because it is obtainable from mass concentration measurements, which are more common than PNSD measurements. Both factors can be easily aquired, which makes the parameterization more practical.

According to the relationship between K_{ex} and aerosol volume concentration and the exponential correlation between K_{ex} and RH, the multiple regression scheme can be set up as follows:

$$K_{ex} = k \times V^{a} \times (1 - \mathrm{RH})^{-b \cdot \mathrm{RH}}, \quad (10)$$

where the units of K_{ex}, V and RH are Mm^{-1}, $\mu\mathrm{m}^3\,\mathrm{cm}^{-3}$ and %, respectively. The parameter k stands for the average K_{ex-vol}, with a unit of $\mathrm{Mm}^{-1}\,(\mu\mathrm{m}^3\,\mathrm{cm}^{-3})^{-1}$.

To simplify calculations, Eq. (10) can be converted into a logarithmic format:

$$\lg(K_{ex}) = b0 + b1 \times \lg V + b2 \times (\mathrm{RH} \times \lg(1 - \mathrm{RH})) \quad (11)$$

Apparently, $b1$ and $b2$ in the Eq. (11) are equal to the exponents of a and $-b$ in the Eq. (10), while k is equivalent to 10^{b0}.

3230 valid data records are taken account into the regression analysis, excluding 63 records during a fog period. An F-test was applied with a confidence level of 95 % (α =

ACPD
11, 31363–31399, 2011

0.05). Regression results show that most of the data input are within the confidence level. The coefficients in Eq. (9) and the correlation coefficient of determination R^2 (Table 3) can be derived from the calculated regression coefficients [$b0b1b2$], after eliminating the records that fell outside the confidence range. To test the reliability, a comparison between the K_{ex} calculated from the regression and that derived from in-situ measured visibilities is made in a log scale.

The regression coefficient a (the exponent of the aerosol volume concentration) is less than 1.0 ($a = 0.944$), which indicates a nonlinear correlation between K_{ex} and aerosol volume concentration, revealing the influence of PNSD patterns on K_{ex}. This also confirms the conclusion of Sect. 4.3.2.

Figure 6 shows the comparison between the regressed and the measured K_{ex}, with the 1 : 1 line displayed in black and the linear fitting line in red. The dispersion degree of K_{ex} below 3000 Mm^{-1} ($lg(K_{ex}) < 3.0$) is low. A strong correlation exists between the K_{ex} and the volume concentration at RH below 90 %. K_{ex} higher than 3000 Mm^{-1} ($lg(K_{ex}) > 3.0$) are more scattered, with the corresponding RH mostly higher than 90 %. This indicates that aerosol hygroscopic growth at high RH can greatly influence the variation of K_{ex}. Nevertheless, the values are all distributed near the 1 : 1 line, with a linear fitting slope of 1.0. Obviously, K_{ex} measurements agree well with the calculated values, because they were also applied in the optimal fitting.

On the other hand, the regression equation shows certain deviations. The corresponding correlation coefficient of determination R^2 is 0.88. It is slightly higher than that of the comparison results between ambient PNSD calculated K_{ex} and measured values in Sect. 4.2 ($R^2 = 0.87$). This deviation might have occured due to the different calculation processes. The K_{ex} calculated from the regression is only influenced by the measured RH and aerosol volume concentration. However, uncertainties of the average size-resolved hygroscopic growth factors, refractive indices, RH and PNSD measurements (both particle size and number concentration) all contribute to the deviations of the K_{ex} calculated from ambient PNSDs.

ACPD
11, 31363–31399, 2011

The good agreement between the K_{ex} calculated from the regression equation and that derived from measured visibilities confirms that the parameterization of K_{ex} with RH and aerosol volume concentration is reliable. Taking advantage of the widespread measurements of aerosol mass concentration in China, the aerosol volume concentration can be easily used to predict these low visibility events. Furthermore, the hygroscopic growth factors of more hygroscopic particles were reported to be relatively constant at high RH conditions during the HaChi summer campaign (Liu et al., 2011), which makes the parameterization scheme widely applicable.

5 Summary and conclusions

Most of the low visibility conditions (VIS < 10 km) in the NCP are accompanied with haze due to the concurrence of high aerosol loading and strong hygroscopic growth at high relative humidity (RH). To reduce the costs of low-visibility-related accidents and to increase the efficiency of transportation, parameterization of low visibilities on hazy days is important. Understanding the controlling factors of low visibility in the NCP is critical to develop a parameterization of low-visibility conditions. Based on the in-situ measured visibility, relative humidity, particle number size distribution (PNSD) and size-resolved hygroscopic growth factors during the HaChi summer campaign, the sensitivity of visibility to RH, aerosol volume concentration and PNSD patterns is studied with the Mie model. A parameterization scheme for low visibilities under hazy conditions is also proposed.

Field observations report that the average aerosol number (of particles larger than 100 nm) and volume concentrations exceed 5300 cm^{-3} and 70 μm^3 cm^{-3}, respectively. The effective radii are mainly distributed in the range of 104–437 nm, with a mean value of 191.8 nm. In-situ measured size-resolved hygroscopic growth factors of particles ranging from 50 nm–1 µm are higher than those of the other particle sizes. Deviations of hygroscopic growth factors for different particle size are larger when RH level is higher. At 99 % RH, the hygroscopic growth factors of particles larger than 30 nm are

ACPD
11, 31363–31399, 2011

all higher than 2.0, and those of particles ranging from 200 nm–1 µm even exceed 3.0, suggesting strong aerosol hygroscopic growth in the NCP. During the summer campaign, about 90 % of the visibility records are below 10 km, and over half of the visibility records are lower than 3 km. Over 90 % of the visibility data are below 5 km, when the aerosol volume concentrations exceeds 75 $\mu m^3\,cm^{-3}$ or when RH > 90 %. These results indicate that the low visibility events are of high frequency in the NCP.

The observational data and measured size-resolved hygroscopic growth factors have been confirmed to be reliable by the good agreement between the extinction coefficients (K_{ex}) calculated from ambient PNSDs and that derived from measured visibilities. The differences existing in the comparisons can be attributed to the possible uncertainties in the measurements of visibility, RH and PNSDs, as well as the deviations of the K_{ex} calculation with the Mie model.

Low visibility events can easily occur due to the high aerosol loading and strong hygroscopic growth in the NCP. Sensitivity studies show that the aerosol volume concentration determines the variation of K_{ex} at RH < 90 %. The relative humidity becomes the dominant influencing factor of K_{ex} at RH > 90 %. In most cases, visibility degradation is caused by the concurrence of aerosol pollution and aerosol hygroscopic growth at high relative humidity. In-situ observations reveal that aerosol volume concentrations above 200 $\mu m^3\,cm^{-3}$ are scarce. Extremely low visibilities (VIS < 1 km) can also happen at low aerosol volume concentration, which reveals the crucial influence of aerosol hygroscopic growth on visibility impairment.

The sensitivity of K_{ex} to PNSD patterns is tested by introducing the concept of extinction coefficient at unit aerosol volume concentration (K_{ex-vol}). Results show that the PNSD pattern has little influence on the K_{ex-vol} at low relative humidity (RH < 80 %). The variation of the relative deviation between the 95th and the 5th K_{ex-vol} is below 1 %. At RH > 80 %, PNSD patterns may slightly influence the K_{ex-vol}, with a largest relative deviation of 2.5 %.

The relative humidity can influence aerosol optical properties, as the size-resolved hygroscopic growth factor of ambient aerosols is closely related to the relative humidity.

ACPD
11, 31363–31399, 2011

The measurements of aerosol mass concentration have been conducted all over China for many years. The aerosol volume concentration can be easily derived from the measured aerosol mass concentrations, which can be applied combined with RH measurements in the prediction of low visibilities. The parameterization scheme of low visibilities is confirmed to be reliable ($R^2 = 0.88$), with good agreement between the K_{ex} calculated from the regression equation and the measured values.

Acknowledgements. This work is supported by the China 973 Program 2011CB403402, the National Natural Science Foundation of China (NSFC) under Grant No. 40875001, 40975083, and the German Science Foundation under grant DFG WI1449/14-1. The Basic Research Fund of Chinese Academy of Meteorological Sciences (2008Z011) also partially supported this work on visibility.

References

Anderson, T. L., Charlson, R. J., Schwartz, S. E., Knutti, R., Boucher, O., Rodhe, H., and Heintzenberg, J.: Climate forcing by aerosols – a hazy picture, Science, 300, 1103–1104, 2003.

Andreae, M. O., Schmid, O., Yang, H., Chand, D., Yu, J. Z., Zeng, L. M., and Zhang, Y. H.: Optical properties and chemical composition of the atmospheric aerosol in urban Guangzhou, China, Atmos. Environ., 42, 6335–6350, 2008.

Sorooshian, A., Hersey, S., Brechtel, F. J., Corless, A., Flagan, R. C., and Seinfeld, J. H.: Rapid, size-resolved aerosol hygroscopic growth measurements: Differential Aerosol Sizing and Hygroscopicity Spectrometer Probe (DASH-SP), Aerosol Sci. Tech., 42, 445–464, 2008.

Bergin, M. H., Cass, G. R., Xu, J., Fang, C., Zeng, L. M., Yu, T., Salmon, L. G., Kiang, C. S., Tang, X. Y., Zhang, Y. H., and Chameides, W. L.: Aerosol radiative, physical, and chemical properties in Beijing during June 1999, J. Geophys. Res.-Atmos., 106(D16), 17969–17980, 2001.

Birmili, W., Stratmann, F., and Wiedensohler, A.: Design of a DMA-based size spectrometer for a large particle size range and stable operation, J. Aerosol Sci., 30(4), 549–533, 1999.

Birmili, W., Wiedensohler, A., Heintzenberg, J., and Lehmann, K.: Atmospheric particle number

ACPD

11, 31363–31399, 2011

size distribution in Central Europe: statistical relations to air masses and meteorology, J. Geophys. Res., 106(D23), 32005–32018, 2001.
Bohren, C. F. and Huffman, D. R.: Absorption and Scattering of Light by Small Particles, John Wiley, Hoboken, 477–482, 1983.
Chang, D., Song, Y., and Liu, B.: Visibility trends in six megacities in China 1973–2007. Atmos. Res., 94, 161–167, 2009.
Cheng, Y. F., Eichler, H., Wiedensohler, A., Heintzenberg, J., Zhang, Y. H., Hu, M., Herrmann, H., Zeng, L. M., Liu, S., Gnauk, T., Brüggemann, E., and He, L. Y.: Mixing state of elemental carbon and non-light-absorbing aerosol components derived from in situ particle optical properties at Xinken in Pearl River Delta of China, J. Geophys. Res., 111, D20204, doi:10.1029/2005JD006929, 2006.
Cheng, Y. F., Wiedensohler, A., Eichler, H., Su, H., Gnauk, T., Bruggemann, E., Herrmann, H., Heintzenberg, J., Slanina, J., Tuch, T., Hu, M., and Zhang, Y. H.: Aerosol optical properties and related chemical apportionment at Xinken in Pearl River Delta of China, Atmos. Environ., 42, 6351–6372, 2008a.
Cheng, Y. F., Heintzenberg, J., Wehner, B., Wu, Z. J., Su, H., Hu, M., and Mao, J. T.: Traffic restrictions in Beijing during the Sino-African Summit 2006: aerosol size distribution and visibility compared to long-term in situ observations, Atmos. Chem. Phys., 8, 7583–7594, doi:10.5194/acp-8-7583-2008, 2008b.
Covert, D. S., Charlson, R. J., and Ahlquist, N. C.: A study of the relationship of chemical composition and humidity to light scattering by aerosols, J. Appl. Meteorol., 11, 968–976, 1972.
Crosby, J. D.: Visibility sensor accuracy: what's realistic? in: 12th Symposium on Meteorological Observations and Instrumentation, Long Beach, CA, 13 February 2003, 2003.
Deng, X., Tie, X., Wu, D., Zhou, X., Bi, X., Tan, H., Li, F., and Jiang, C.: Long-term trend of visibility and its characterizations in the Pearl River Delta (PRD) region, China, Atmos. Environ., 42, 1424–1435, 2008.
Deng, Z. Z., Zhao, C. S., Zhang, Q., Huang, M. Y., and Ma, X. C.: Statistical analysis of microphysical properties and the parameterization of effective radius of warm clouds in Beijing area, Atmos. Res., 93, 888–896, 2009.
Deng, Z. Z., Zhao, C. S., Ma, N., Liu, P. F., Ran, L., Xu, W. Y., Chen, J., Liang, Z., Liang, S., Huang, M. Y., Ma, X. C., Zhang, Q., Quan, J. N., Yan, P., Henning, S., Mildenberger, K., Sommerhage, E., Schäfer, M., Stratmann, F., and Wiedensohler, A.: Size-resolved and bulk

ACPD
11, 31363–31399, 2011

activation properties of aerosols in the North China Plain, Atmos. Chem. Phys., 11, 3835–3846, doi:10.5194/acp-11-3835-2011, 2011.
Eichler, H., Cheng, Y. F., Birmili, W., Wiedensohler, A., Brüggemann, E., Gnauk, T., Herrmann, H., Althausen, D., Ansmann, A., Engelmann, R., Tesche, M., Zhang, Y. H., Hu, M., Liu, S., Zeng, L. M.: Hygroscopic properties and ambient extinction of aerosol particles in South-Eastern China, Atmos. Environ., 42, 6321–6334, doi:10.1016/j.atmosenv.2008.05.007, 2008.
FD12P User Guide in English: available at: http://www.vaisala.com/VaisalaDocuments/UserGuidesandQuickRefGuides/FD12PUserGuideinEnglish.pdf, last access: 25 November 2011.
Hidy, G. M.: Surface-level fine particle mass concentrations: from hemispheric distributions to megacity sources, J. Air Waste Manage. Assoc., 59, 770–789, 2009.
Hoyle, C. R., Myhre, G., and Isaksen, I. S. A.: Present-day contribution of anthropogenic emissions from China to the global burden and radiative forcing of aerosol and ozone, Tellus B, 61, 618–624, 2009.
Hussein, T., Dal Maso, M., Petäjä, T., Koponen, I. K., Paatero, P., Aalto, P. P., Hämeri, K., and Kulmala, M.: Evaluation of an automatic algorithm for fitting the particle number size distributions, Boreal Environ. Res., 10(5), 337–355, 2005.
Hyslop, N. P.: Impaired visibility: the air pollution people see, Atmos. Environ., 43, 182–195, 2009.
Lesins, G., Chylek, P., Lohman, U.: A study of internal and external mixing scenarios and its effect on aerosol optical properties and direct radiative forcing. J. Geophys. Res., 107 (D10), 4094, 2002.
Liu, P. F., Zhao, C. S., Göbel, T., Hallbauer, E., Nowak, A., Ran, L., Xu, W. Y., Deng, Z. Z., Ma, N., Mildenberger, K., Henning, S., Stratmann, F., and Wiedensohler, A.: Hygroscopic properties of aerosol particles at high relative humidity and their diurnal variations in the North China Plain, Atmos. Chem. Phys., 11, 3479–3494, doi:10.5194/acp-11-3479-2011, 2011.
Liu, P., Zhao, C., Zhang, Q., Deng, Z., Huang, M., Ma, X., and Tie, X.: Aircraft study of aerosol vertical distributions over Beijing and their optical properties, Tellus B, 61, 756–767, 2009.
Ma, N., Zhao, C. S., Müller, T., Cheng, Y. F., Liu, P. F., Deng, Z. Z., Xu, W. Y., Ran, L., Nekat, B., van Pinxteren, D., Gnauk, T., Müller, K., Herrmann, H., Yan, P., Zhou, X. J., and Wiedensohler, A.: A new method to determine the mixing state of light absorbing carbonaceous using the measured aerosol optical properties and number size distributions, Atmos. Chem.

ACPD
11, 31363–31399, 2011

Phys. Discuss., 11, 27475–27519, doi:10.5194/acpd-11-27475-2011, 2011a.
Ma, N., Zhao, C. S., Nowak, A., Müller, T., Pfeifer, S., Cheng, Y. F., Deng, Z.Z., Liu, P. F., Xu, W. Y., Ran, L., Yan, P., Göbel, T., Hallbauer, E., Mildenberger, K., Henning, S., Yu, J., Chen, L. L., Zhou, X. J., Stratmann, F., and Wiedensohler, A.: Aerosol optical properties in the North China Plain during HaChi campaign: an in-situ optical closure study, Atmos. Chem. Phys., 11, 5959–5973, doi:10.5194/acp-11-5959-2011, 2011b.
Mie, G.: Beiträge zur optic trüber Medien speziell kolloidaler Metallösungen, Ann. Phys., 25, 377–445, 1908.
Motallebi, N. and Cahill, T. A.: Influence of particulate size on statistical studies of visibility at California regions, Atmosfera, 3, 111–126, 1990.
Ouimette, J. R. and Flagan, R. C.: The extinction coefficient of multicomponent aerosols, Atmos. Environ., 16, 2405–2419, 1982.
Pan, X. L., Yan, P., Tang, J., Ma, J. Z., Wang, Z. F., Gbaguidi, A., and Sun, Y. L.: Observational study of influence of aerosol hygroscopic growth on scattering coefficient over rural area near Beijing mega-city, Atmos. Chem. Phys., 9, 7519–7530, doi:10.5194/acp-9-7519-2009, 2009.
Petters, M. D. and Kreidenweis, S. M.: A single parameter representation of hygroscopic growth and cloud condensation nucleus activity, Atmos. Chem. Phys., 7, 1961–1971, doi:10.5194/acp-7-1961-2007, 2007.
Quinn, P. K. and Bates, T.: North American, Asian, and Indian haze: similar regional impacts on climate?, Geophys. Res. Lett., 30, 1555, 2003.
Randles, C. A., Russell, L. M., and Ramaswamy, V.: Hygroscopic and optical properties of organic sea salt aerosol and consequences for climate forcing, Geophys. Res. Lett., 31, L16108, doi:10.1029/2004GL020628, 2004.
Seinfeld, J. H. and Pandis, S. N.: Atmospheric Chemistry and Physics, John Wiley & Sons, Inc., New York, 1998.
Sloane, C. S.: Optical properties of aerosols – comparison of measurements with model calculations, Atmos. Environ., 17, 409–416, 1983.
Sloane, C. S.: Optical properties of aerosols of mixed composition, Atmos. Environ., 18, 871–878, 1984.
Stock, M., Cheng, Y. F., Birmili, W., Massling, A., Wehner, B., Müller, T., Leinert, S., Kalivitis, N., Mihalopoulos, N., and Wiedensohler, A.: Hygroscopic properties of atmospheric aerosol particles over the Eastern Mediterranean: implications for regional direct radiative forcing under clean and polluted conditions, Atmos. Chem. Phys., 11, 4251–4271, doi:10.5194/acp-

ACPD
11, 31363–31399, 2011

11-4251-2011, 2011.
Swietlicki, E., Hansson, H.-C., Hämeri, K., Svenningsson, B., Massling, A., McFiggans, G., McMurry, P. H., Petäjä, T., Tunved, P., Gysel, M., Topping, D., Weingartner, E., Baltensperger, U., Rissler, J., Wiedensohler, A., and Kulmala, M.: Hygroscopic properties of submicrometer atmospheric aerosol particles measured with H-TDMA instruments in various environments: a review, Tellus B, 60, 432–469, 2008.
Wehner, B., Birmili, W., Ditas, F., Wu, Z., Hu, M., Liu, X., Mao, J., Sugimoto, N., and Wiedensohler, A.: Relationships between submicrometer particulate air pollution and air mass history in Beijing, China, 2004–2006, Atmos. Chem. Phys., 8, 6155–6168, doi:10.5194/acp-8-6155-2008, 2008.
Wen, C.-C. and Yeh, H.-H.: Comparative influences of airborne pollutants and meteorological parameters on atmospheric visibility and turbidity, Atmos. Res., 96, 496–509, 2010.
Wex, H.: Closure and sensitivity studies on physical parameters of rural continental aerosols, Ph. D. Thesis, Leipzig University, 2002.
Wex, H., Neusüß, C., Wendisch, M., Stratmann, F., Koziar, C., Keil, A., Wiedensohler, A., and Ebert, M.: Particle scattering, backscattering, and absorption coefficients: An in situ closure and sensitivity study, J. Geophys. Res., 107(D21), 8122, doi:10.1029/2000JD000234, 2002.
Whitby, K. T.: The physical characteristics of sulfur aerosols, Atmos. Environ., 12, 135–159, 1978.
Wiedensohler, A., Birmili, W., Nowak, A., Sonntag, A., Weinhold, K., Merkel, M., Wehner, B., Tuch, T., Pfeifer, S., Fiebig, M., Fjäraa, A. M., Asmi, E., Sellegri, K., Depuy, R., Venzac, H., Villani, P., Laj, P., Aalto, P., Ogren, J. A., Swietlicki, E., Roldin, P., Williams, P., Quincey, P., Hüglin, C., Fierz-Schmidhauser, R., Gysel, M., Weingartner, E., Riccobono, F., Santos, S., Grüning, C., Faloon, K., Beddows, D., Harrison, R. M., Monahan, C., Jennings, S. G., O'Dowd, C. D., Marinoni, A., Horn, H.-G., Keck, L., Jiang, J., Scheckman, J., McMurry, P. H., Deng, Z., Zhao, C. S., Moerman, M., Henzing, B., and de Leeuw, G.: Particle mobility size spectrometers: harmonization of technical standards and data structure to facilitate high quality long-term observations of atmospheric particle number size distributions, Atmos. Meas. Tech. Discuss., 3, 5521–5587, doi:10.5194/amtd-3-5521-2010, 2010.
Wu, D., Tie, X., Li, C., Ying, Z., Kai-Hon Lau, A., Huang, J., Deng, X., and Bi, X.: An extremely low visibility event over the Guangzhou region: a case study, Atmos. Environ., 39, 6568–6577, 2005.
Xu, W. Y., Zhao, C. S., Ran, L., Deng, Z. Z., Liu, P. F., Ma, N., Lin, W. L., Xu, X. B., Yan, P.,

ACPD
11, 31363–31399, 2011

He, X., Yu, J., Liang, W. D., and Chen, L. L.: Characteristics of pollutants and their correlation to meteorological conditions at a suburban site in the North China Plain, Atmos. Chem. Phys., 11, 4353–4369, doi:10.5194/acp-11-4353-2011, 2011.

Yan, P., Pan, X. L., Tang, J., Tang, J., Zhou, X. J., and Zeng, L. M.: An experimental study on the influence of relative humidity on the atmospheric aerosol scattering coefficient at an urban site in Beijing, Acta Meteorol. Sin., 6(1), 11–119, 2008a.

Yan, P., Tang, J., Huang, J., Mao, J. T., Zhou, X. J., Liu, Q., Wang, Z. F., and Zhou, H. G.: The measurement of aerosol optical properties at a rural site in Northern China, Atmos. Chem. Phys., 8, 2229–2242, doi:10.5194/acp-8-2229-2008, 2008b.

Yang, F., Tan, J., Zhao, Q., Du, Z., He, K., Ma, Y., Duan, F., Chen, G., and Zhao, Q.: Characteristics of $PM_{2.5}$ speciation in representative megacities and across China, Atmos. Chem. Phys., 11, 5207–5219, doi:10.5194/acp-11-5207-2011, 2011.

Ye, B. M., Ji, X. L., Yang, H. Z., Yao, X. H., Chan, C. K., Cadle, S. H., Chan, T., and Mulawa, P. A.: Concentration and chemical composition of $PM_{2.5}$ in Shanghai for a 1-year period, Atmos. Environ., 37(4), 499–510, 2003.

Yu, H., Wu, C., Wu, D., and Yu, J. Z.: Size distributions of elemental carbon and its contribution to light extinction in urban and rural locations in the pearl river delta region, China, Atmos. Chem. Phys., 10, 5107–5119, doi:10.5194/acp-10-5107-2010, 2010.

Zhang, Q. H., Zhang, J. P., and Xue, H. W.: The challenge of improving visibility in Beijing, Atmos. Chem. Phys., 10, 7821–7827, doi:10.5194/acp-10-7821-2010, 2010.

Zhao, C., Tie, X., Brasseur, G., Noone, K. J., Nakajima, T., Zhang, Q., Zhang, R., Huang, M., Duan, Y., Li, G., and Ishizaka, Y.: Aircraft measurements of cloud droplet spectral dispersion and implications for indirect aerosol radiative forcing, Geophys. Res. Lett., 33, L16809, doi:10.1029/2006gl026653, 2006a.

Zhao, C., Tie, X., and Lin, Y.: A possible positive feedback of reduction of precipitation and increase in aerosols over Eastern Central China, Geophys. Res. Lett., 33, L11814, doi:10.1029/2006gl025959, 2006b.

ACPD
11, 31363–31399, 2011

Table 1. Frequencies (Freq) of different visibility ranges.

VIS (km)	Freq (%)
< 1	13
1–3	41.5
3–5	19.2
5–10	15.8
> 10	10.5

ACPD
11, 31363–31399, 2011

Table 2. Characteristics of VIS, N, S, V, R_{eff} and RH.

Parameter	Min	Max	Mean	Std
VIS (km)	0.021	33.032	4.145	4.040
N (10^3 cm^{-3})	3.35	51.06	17.17	5.91
N^*_{100} (10^3 cm^{-3})	0.50	15.72	5.32	2.55
S (μm^2 cm^{-3})	94.45	3053.55	1071.90	548.34
V (μm^3 cm^{-3})	4.51	233.89	70.94	41.97
R_{eff} (nm)	104.9	437.1	191.8	24.0
RH (%)	28.2	100.0	81.6	15.7

* N_{100} represents the number concentration of particles larger than 100 nm.

ACPD
11, 31363–31399, 2011

Table 3. Regression coefficients of the parameterization scheme.

Coefficient	Value
k	29.309
a	0.944
b	−0.475
R^2	0.88

ACPD
11, 31363–31399, 2011

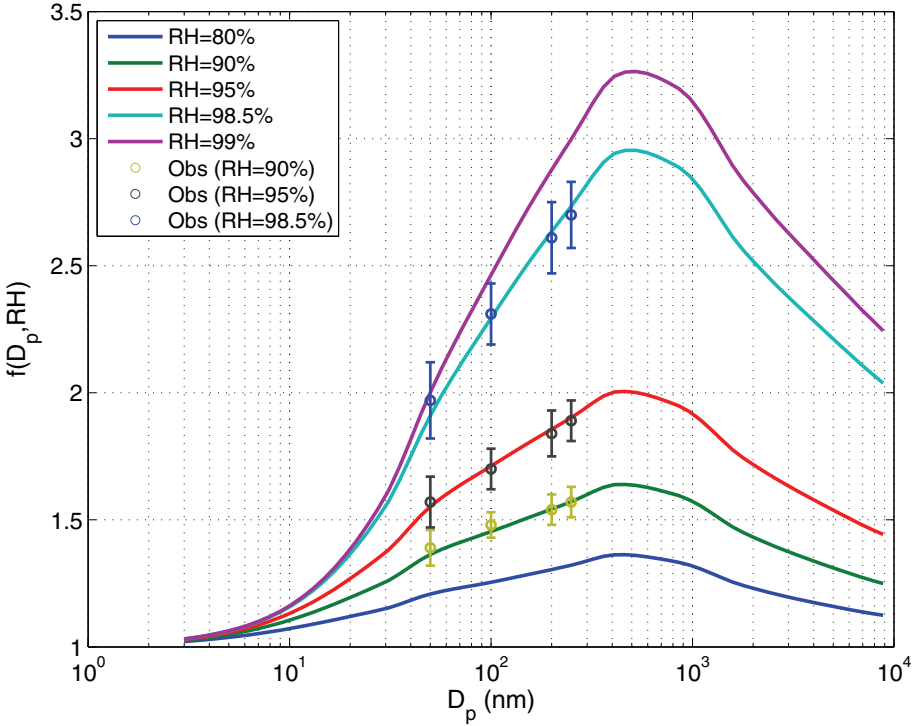

Fig. 1. Size-resolved hygroscopic growth factors at 80 %, 90 %, 95 %, 98.5 % and 99 % RH (displayed in colored lines). Colored circles represent the corresponding mean values of measured hygroscopic growth factors of aerosol particles (with different dry diameters of 50, 100, 200 and 250 nm) at set RHs (90 %, 95 % and 98.5 %, respectively) during HaChi summer campaign; the error bars represent ±1 standard deviation. (Liu et al., 2011).

ACPD
11, 31363–31399, 2011

A parameterization of low visibilities for hazy days in the North China Plain

J. Chen et al.

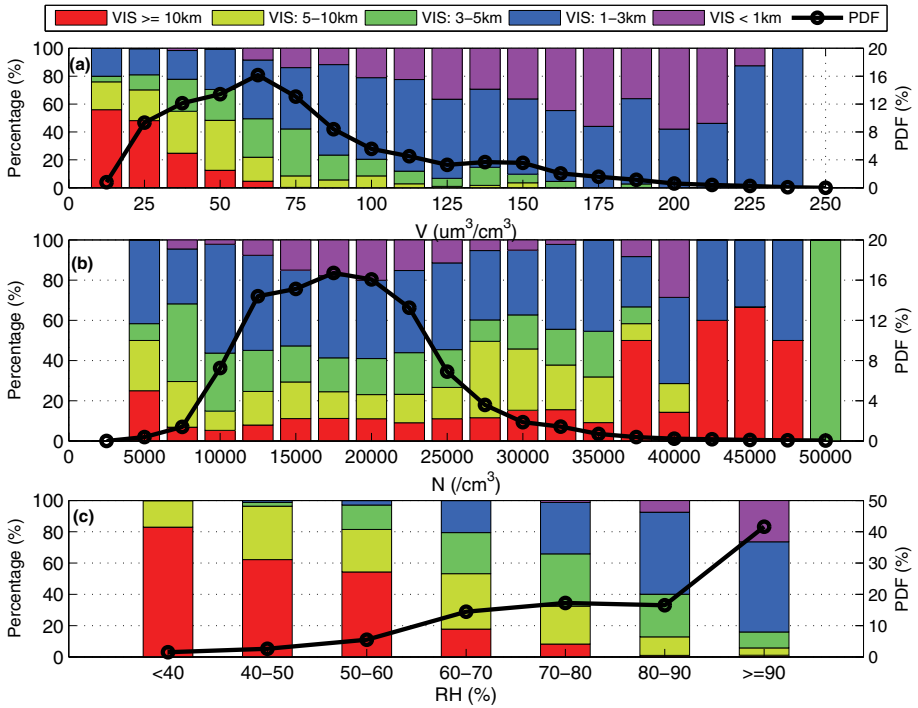

Fig. 2. Percentages of five specific visibility groups at different aerosol **(a)** volume concentration (V), **(b)** number concentration (N) and corresponding **(c)** RH ranges, as well as their corresponding probability distribution functions (PDF) presented in dotted dark lines; the colored bars stand for the situation of corresponding visibility groups (VIS >= 10 km, 5 km =< VIS < 10 km 3 km =< VIS < 5 km, 1 km =< VIS < 3 km and VIS < 1 km).

ACPD
11, 31363–31399, 2011

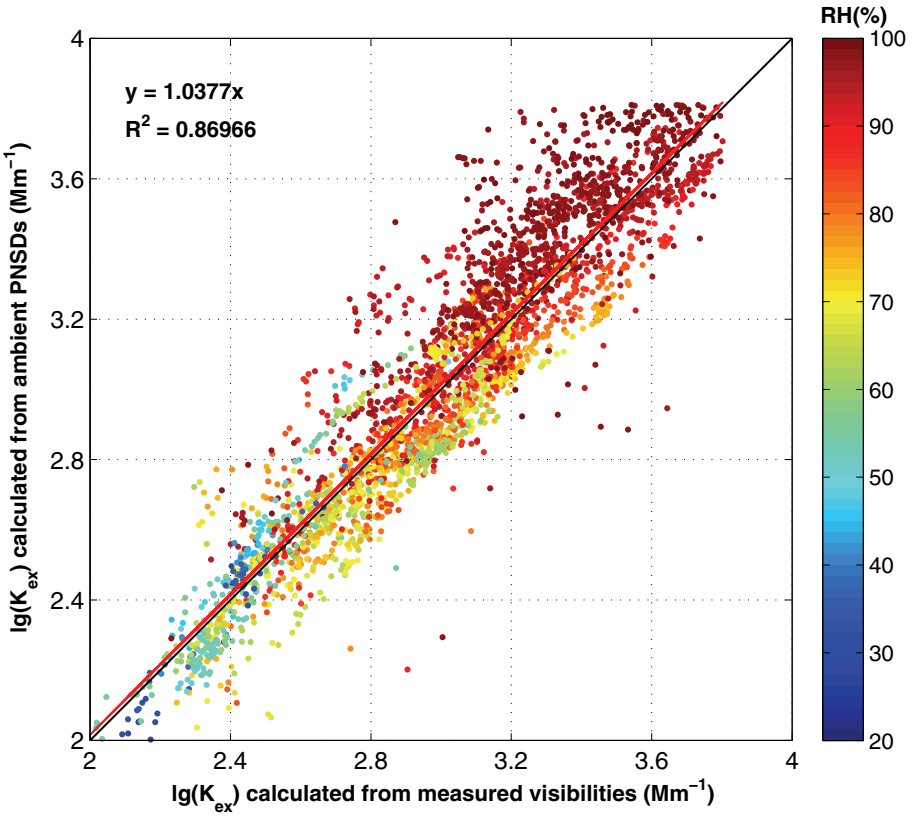

Fig. 3. Comparison of K_{ex} between calculated from ambient PNSDs and measured ones at log scale coordinates. Colored dots stand for the corresponding RH.

ACPD
11, 31363–31399, 2011

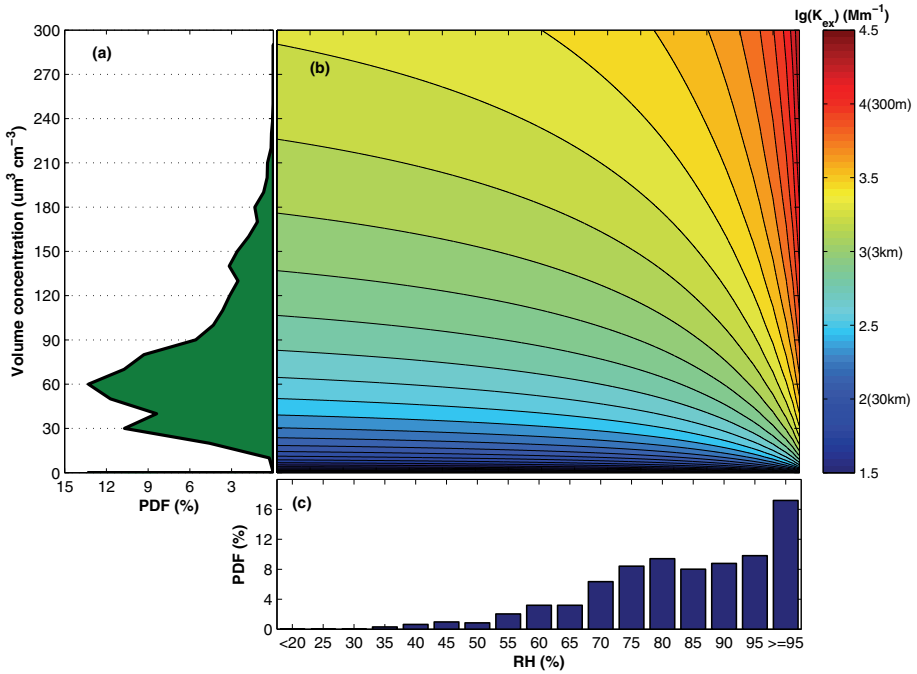

Fig. 4. (b) Calculated K_{ex} at given aerosol volume concentrations and RH at logarithmic scale; **(a)** and **(c)** PDFs of measured aerosol volume concentrations and RH, respectively.

ACPD
11, 31363–31399, 2011

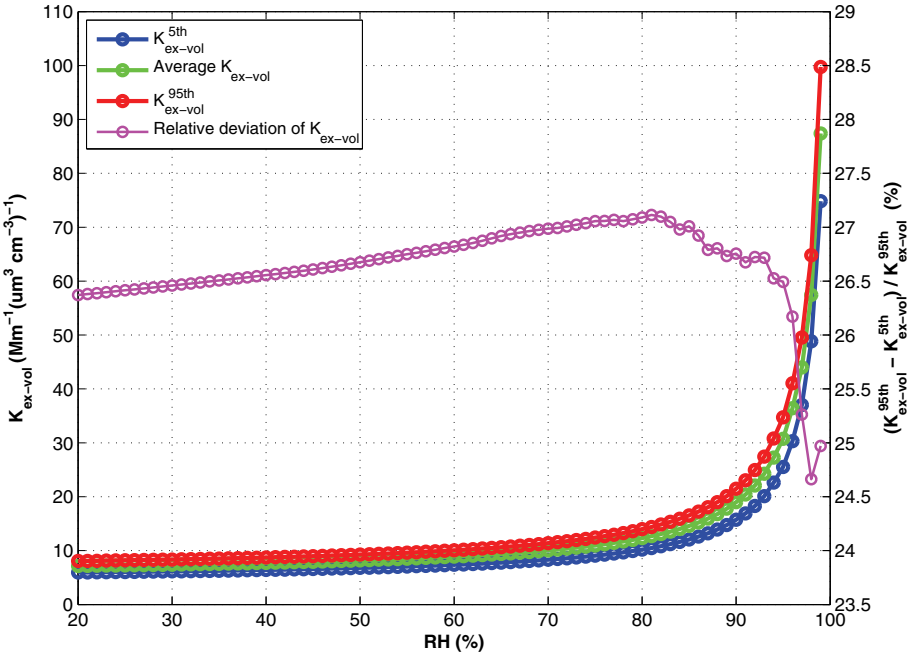

Fig. 5. Variation of the aerosol volume extinction coefficients (K_{ex-vol}) with RH. Green, blue and red circled lines stand for the average, the 5th and the 95th percentiles of the volume extinction coefficients (K^{5th}_{ex-vol} and K^{95th}_{ex-vol}). The magenta line represents the relative deviations of K_{ex-vol}, which is defined as $(K^{95th}_{ex-vol} - K^{5th}_{ex-vol})/K^{95th}_{ex-vol}$.

ACPD
11, 31363–31399, 2011

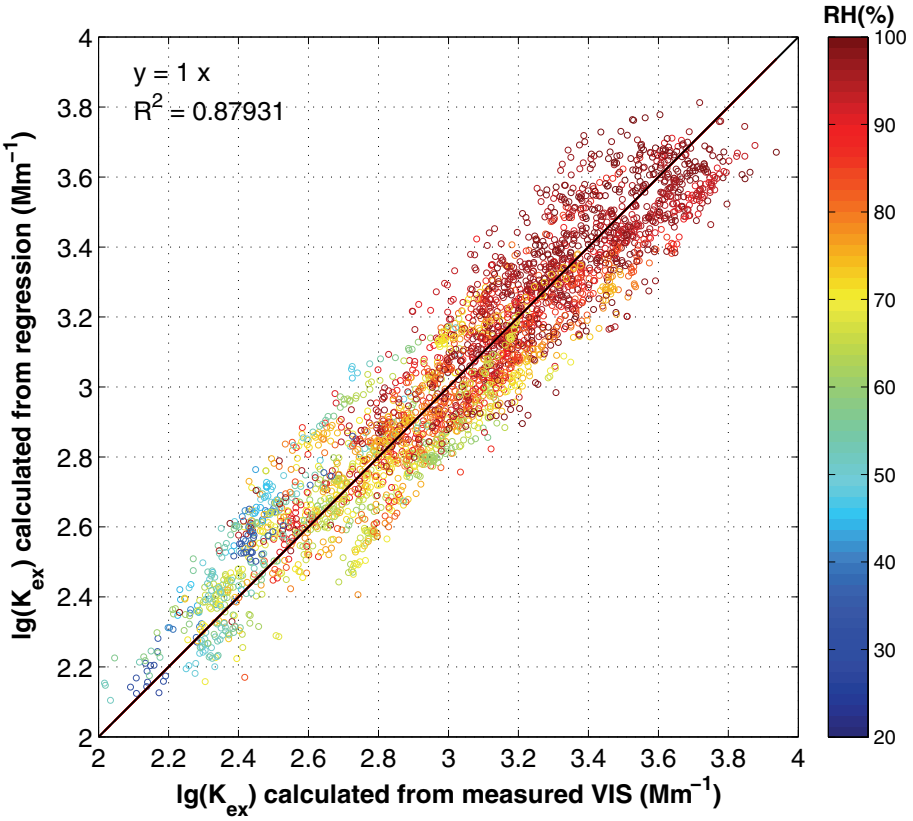

Fig. 6. Comparison results of ten-minute average K_{ex} between calculated from regression equation and measured visibilities; the colored circles stand for the corresponding RHs, which increase with color from blue to red.

ACPD
11, 31363–31399, 2011